



ELSEVIER

Journal of Chromatography A, 796 (1998) 239–248

---

---

JOURNAL OF  
CHROMATOGRAPHY A

---

---

## Simulated moving bed chromatographic resolution of a chiral antitussive

Eric Francotte<sup>a</sup>, Paul Richert<sup>a</sup>, Marco Mazzotti<sup>b</sup>, Massimo Morbidelli<sup>c,\*</sup>

<sup>a</sup>Pharmaceutical Research, K-122.P.25 Novartis Pharma AG, CH-4002 Basel, Switzerland

<sup>b</sup>ETH Zürich, Institut für Verfahrenstechnik Sonneggstrasse 3, CH-8092 Zürich, Switzerland

<sup>c</sup>ETH Zürich, Laboratorium für Technische Chemie, Universitätstrasse 6, CH-8092 Zürich, Switzerland

Received 29 July 1997; received in revised form 24 September 1997; accepted 25 September 1997

---

### Abstract

The behavior of a laboratory simulated moving bed (SMB) unit for continuous chromatographic separation of enantiomers has been considered. This was applied to the resolution of a chiral antitussive agent, guaifenesin, on Chiralcel OD, during an experimental campaign involving nineteen runs. The application of recently developed criteria for the design and optimization of SMB units allows us to understand and rationalize the experimental results, as well as to indicate how to optimize the separation performances. A three-step procedure to determine the adsorption isotherms needed to apply these criteria is proposed; it is reliable and may be applied also where pure components are not available. © 1998 Elsevier Science B.V.

*Keywords:* Enantiomer separation; Simulated moving bed chromatography; Preparative chromatography; Guaifenesin

---

### 1. Introduction

The application of simulated moving beds (SMB) [1] for the preparative and production scale separation of fine chemical and pharmaceutical products, and in particular enantiomers, is gaining increasing importance. One of the key features of the success of chromatographic techniques with respect to asymmetric synthesis for pure enantiomer production is the possibility of developing the separation within short times by scaling up directly the high-performance liquid chromatography (HPLC) analytical method, which is in most cases available in the laboratory during the development of a new product.

In addition, since the SMB technology applies the chromatographic principle in a continuous fashion, it allows the achievement of valuable improvements in terms of solvent consumption and specific productivity with respect to classical batchwise preparative chromatography [2,3]. Therefore, this technique allows the reduction of development times and production costs of a new drug, increasing at the same time the availability of both enantiomers. Until now several applications of SMBs to the resolution of racemates have been reported in the literature [4–12].

SMB units typically operate under overload conditions, which allow achievement of the above mentioned performance improvements but lead to nonlinear competitive adsorption behavior. These can be accounted for when selecting the operating

---

\*Corresponding author. Tel.: +41 1 6323034; fax: +41 1 6321082.

conditions, i.e., feed concentration, switching time and internal fluid flow-rates, by following the design criteria recently presented [13,14]. These allow the determination of regions in the operating parameter space corresponding to different separation regimes and evaluation of the optimal operating conditions for the desired separation. Their usefulness has been demonstrated through comparison of theoretical predictions with different sets of experimental results.

In this work, this approach is used to analyse the performances achieved in a commercial SMB unit during an experimental campaign for the separation of a drug developed in the former Ciba–Geigy laboratories, i.e., the antitussive agent guaifenesin [12]. In such a way, a better understanding and rationalization of the SMB behavior can be achieved. Thus the peculiar features of this separation are clearly explained and hints for its optimization are provided. The adoption of the proposed approach requires some knowledge about the competitive adsorption isotherms of the components to be separated. From the design point of view, this requirement is altogether equivalent to the necessity of providing vapor–liquid equilibrium data in order to apply the McCabe–Thiele method for binary distillation columns. However, measuring multicomponent adsorption isotherms is always a rather difficult task [15]. In particular, in the case of enantiomer separations this is often not possible at all, due to the lack of pure enantiomers in general and to the shortage of the racemate itself in some cases. This implies that some procedure must be devised to determine at least an estimate of the adsorption isotherms through which an approximate but rather reliable region of complete separation in the operating parameter space may be calculated. Several different procedures may be conceived, the specific choice depending not only on the system under examination and the availability of the species to be separated but also on the experimental apparatus available.

In this work a particular procedure is proposed and adopted. This is based on the determination of the approximate isotherms through a few analytical pulse chromatograms of the racemic mixture at increasing pulse concentration, and their refinement through a few ad hoc SMB experiments. This is not meant as a procedure worth applying in any case, but it is certainly useful whenever a SMB unit is available, for the reasons that will be discussed later.

## 2. Experimental

The separation of the enantiomers of guaifenesin on the chiral stationary phase Chiralcel OD (Daicel Chemical, Tokyo, Japan; average particle diameter: 20  $\mu\text{m}$ ) was considered, using heptane–ethanol (65:35, v/v) as mobile phase [12].

### 2.1. Analytical chromatography

The analytical chromatograms were obtained using a HPLC column (length: 25 cm; I.D.: 0.4 cm), containing 1.9 g of chiral stationary phase. Injection loop volume and extra-column dead volume were 20  $\mu\text{l}$  and 392  $\mu\text{l}$ , respectively. All the pulse chromatograms were obtained with a fluid flow-rate of 0.7 ml/min. The operating temperature was 23°C.

### 2.2. SMB unit

The SMB unit was a Sorbex Prep (UOP, Des Plaines, IL, USA), equipped with 16 columns (length: 6 cm; I.D.: 2.1 cm) each containing 12.6 g of chiral stationary phase [12]. The zone configuration adopted was 5–5–5–1 as illustrated in the scheme in Fig. 1. According to the original patent, the flow-rate in the fourth section after the raffinate outlet was zero [16]. Mobile phase and temperature were the same as above. The extra-column dead volume, i.e., 0.31 ml, was negligible with respect to the column

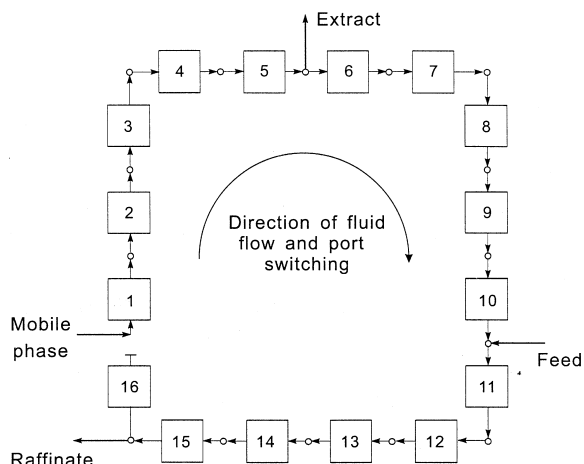


Fig. 1. Scheme of the Sorbex Prep<sup>TM</sup> SMB unit used for the separation of the enantiomers of guaifenesin: a 5–5–5–1 zone configuration with  $Q_4=0$  was adopted [16].

volume, i.e., 20.8 ml. The feed concentration in all the experimental runs was 3% (30 g/l).

### 3. Background

For the sake of clarity, in this section some previously reported results are briefly summarized. These refer to the experimental results achieved during the SMB campaign for the separation of guaifenesin [12] and to the theoretical criteria for the design of operating conditions of SMBs [13,14].

#### 3.1. SMB experimental results

Nineteen SMB experimental runs are considered. Their operating conditions, i.e., switch time,  $t^*$  ( $t^*$  is the time period between two successive switches of the inlet and outlet ports), mobile phase flow-rate fed to section 1 ( $Q_1$ ), extract flow-rate ( $Q_E$ ), and feed flow-rate ( $Q_F$ ), are reported in Table 1. Three different groups are considered: runs F1 to F7 where only the feed flow-rate changes ( $t^*=7.5$  min), runs E1 to E7 where only the extract flow-rate is varied ( $t^*=5$  min) and runs G1 to G5 where two or more

parameters change. It must be noted that from the information in Table 1 and through the overall material balances at the nodes of the unit (see Fig. 1) the internal fluid flow-rates in sections 2 and 3,  $Q_2$  and  $Q_3$ , can be readily calculated as  $Q_2=Q_1-Q_E$  and  $Q_3=Q_2+Q_F$ . In this case the latter parameter coincides with the raffinate flow-rate,  $Q_R$ , since  $Q_4=0$ .

Table 1 indicates also the values of the flow-rate ratios  $m_j$ ,  $j=1,2,3$ , defined as:

$$m_j = \frac{Q_j t^* - V\varepsilon}{V(1 - \varepsilon)}, \quad (1)$$

where  $V=20.8$  ml and  $\varepsilon=0.704$  are the overall volume and void fraction of the single chromatographic column, respectively. The value of the latter parameter was determined as described in Section 4.1.

Finally, the last two columns of Table 1 report the experimental purity values;  $P_E = 100 \times c_A^E / (c_A^E + c_B^E)$  for the extract and  $P_R = 100 \times c_B^R / (c_A^R + c_B^R)$  for the raffinate, where  $c_A$  and  $c_B$  are the concentration of the more and less retained enantiomer respectively. These indicate rather satisfactory separation perform-

Table 1  
Operating conditions and purities of the outlet streams in the experimental runs

Run	Switch time $t^*$ (min)	Flow-rates (ml/min)			Flow-rate ratios			Experimental purity values (%)	
		$Q_1$	$Q_E$	$Q_F$	$m_1$	$m_2$	$m_3$	$P_E$	$P_R$
F1	7.5	5.71	2.50	0.20	4.58	1.54	1.78	99.1	99.9
F2	7.5	5.71	2.50	0.30	4.58	1.54	1.90	99.2	99.9
F3	7.5	5.71	2.50	0.40	4.58	1.54	2.02	99.2	99.7
F4	7.5	5.71	2.50	0.50	4.58	1.54	2.15	99.3	99.7
F5	7.5	5.71	2.50	0.55	4.58	1.54	2.21	99.4	97.6
F6	7.5	5.71	2.50	0.60	4.58	1.54	2.27	99.4	87.0
F7	7.5	5.71	2.50	0.70	4.58	1.54	2.39	99.4	74.8
E1	5.0	7.55	2.40	0.75	3.76	1.81	2.42	99.6	71.3
E2	5.0	7.55	2.55	0.75	3.76	1.69	2.30	99.3	85.7
E3	5.0	7.55	2.75	0.75	3.76	1.52	2.13	99.4	99.1
E4	5.0	7.55	2.85	0.75	3.76	1.44	2.05	99.1	99.1
E5	5.0	7.55	3.05	0.75	3.76	1.28	1.89	99.1	99.4
E6	5.0	7.55	3.35	0.75	3.76	1.04	1.65	90.0	99.5
E7	5.0	7.55	3.55	0.75	3.76	0.87	1.48	72.0	99.6
G1	7.5	5.50	2.30	0.50	4.32	1.52	2.14	99.1	99.7
G2	7.5	5.30	2.10	0.50	4.08	1.52	2.14	99.4	99.7
G3	5.0	7.95	3.15	0.75	4.08	1.52	2.13	99.3	99.6
G4	5.0	7.85	3.05	0.75	4.00	1.52	2.13	99.4	99.3
G5	5.0	7.75	2.95	0.75	3.92	1.52	2.13	99.3	99.2

ance in terms of purities of the outlet streams: in twelve runs out of nineteen (runs F1 to F4, E3 to E5 and G1 to G5) purities are larger than 99% in both extract and raffinate. This corresponds to complete separation, i.e., the two enantiomers are collected separately in the two outlet streams.

By comparing the first and the second group of experiments, it is evident that the effect of changing the feed flow-rate is rather different than that of changing the extract flow-rate. Beside the obvious quantitative differences, there are also qualitative ones. Feed flow-rate changes in runs F1 to F7 have almost no effect on  $P_E$  (which is always above 99%), while on the other hand  $P_R$  drops from 99.9% to 74.8%. In contrast, extract flow-rate changes in runs E1 to E7 affect both outlet purities sharply; when the extract flow-rate increases  $P_E$  decreases whereas  $P_R$  also increases. Finally, it is worth noting that in spite of changes in all the operating parameters (not only flow-rates but also switching time) separation performances are very similar in experimental runs G1 to G5.

In the following a consistent conceptual framework will be provided for the interpretation of all these experimental findings.

### 3.2. Design of the operating conditions

The experimental performances of SMBs can be properly interpreted following a recently presented approach, which leads to some criteria for the choice of operating conditions of SMB units [13,14]. This is done in the frame of equilibrium theory (i.e., neglecting axial dispersion and mass transfer resistances), where it can be proven that the separation performances of SMBs depend on the choice of the flow-rate ratios  $m_j$  in the sections of the unit (these can be either three or four depending on the unit configuration).

These operating parameters are the coordinates of the operating parameter space, which can be divided into four separation regions, each corresponding to a different separation regime. The shape and position of these regions depend on the equilibrium adsorption isotherms of the components to be separated and their feed concentration, i.e.,  $c_A^F$  and  $c_B^F$  (A and B label the more and the less adsorbable species,

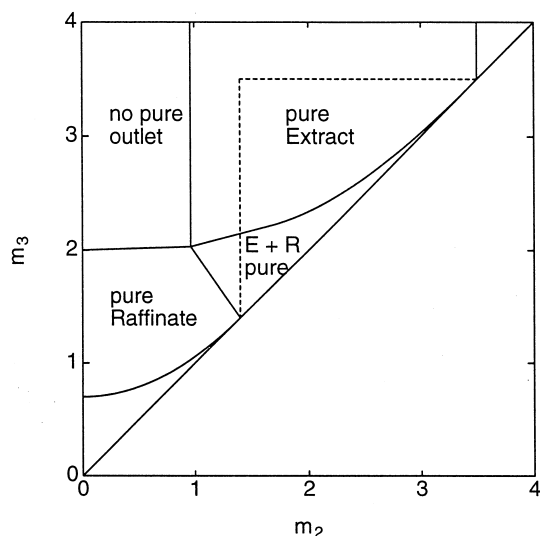


Fig. 2. Separation of a two component mixture using a nonadsorbable desorbent. Regions of the  $(m_2, m_3)$  plane with different separation regimes in terms of purity of the outlet streams, for a system described by the nonstoichiometric Langmuir adsorption isotherm:  $H_A=3.5$ ,  $H_B=1.4$ ,  $K_A=0.0550$  1/g,  $K_B=0.0135$  1/g,  $c_A^F=15$  g/l,  $c_B^F=15$  g/l. Dashed boundaries correspond to the complete separation region for a linear system with the same Henry constants.

respectively, and it is assumed that they are dissolved in the solvent constituting the mobile phase).

This can be best illustrated by Fig. 2, where the projection of the regions of separation on the  $(m_2, m_3)$  plane spanned by the flow-rate ratios of the two key sections of the unit is drawn. The triangle-shaped region is constituted of operating points which in the frame of equilibrium theory allow complete separation to be achieved ( $P_E=P_R=100\%$ ). Above it and on its left hand side there are the pure extract region (where  $P_E=100\%$ , but  $P_R<100\%$ ) and the pure raffinate region (where  $P_R=100\%$ , but  $P_E<100\%$ ), respectively. The fourth region corresponds to purity values of both outlet streams below 100%. It is worth recalling that the separation regions in the  $(m_2, m_3)$  plane can be considered only if the proper constraints on  $m_1$  and  $m_4$  are fulfilled. The former imposes that the flow-rate in section 1 is larger than the Henry constant of component A, i.e.,  $m_1>H_A$ ; the latter requires that the flow-rate ratio in section 4 is smaller than a critical value  $m_{4,cr}$ , which

certainly holds true since the critical value is positive and  $m_4$  is negative due to  $Q_4=0$ .

In the example used to draw Fig. 2 the system is described by the multicomponent Langmuir adsorption equilibrium isotherm. In this case the boundaries of the region of complete separation are given by explicit expressions. This is also the case for modified Langmuir isotherms (where the adsorbed phase concentration is given by the sum of a Langmuir and a linear term) [14]. In the case of bi-Langmuir isotherms (where the adsorbed concentration is given by the sum of two different Langmuirian terms) a similar picture is obtained [17]. This is a rather satisfactory state-of-the-art since by using the above mentioned semi-empirical isotherms it is possible to characterize most enantiomer separations.

The above mentioned approach allows us to account for the well-known phenomenon of the increasing nonlinearity of SMB separations following from increases of feed composition. Increasing feed concentration yields larger and larger productivity, but at the same time less and less accessible and robust complete separation regions [13,14]. This can be observed also in Fig. 2 by comparing the triangle-shaped complete separation region (solid boundaries) with the region with dashed boundaries, which corresponds to complete separation of the same components when infinitely diluted in the feed stream. Under these conditions the system behaves linearly and the complete separation region becomes a square triangle whose position is defined by the Henry constants of the two components to be separated.

It can also be demonstrated that solvent consumption and specific productivity (mass of species separated per unit time and mass of stationary phase) are optimal on the vertex of the complete separation region [13,14].

#### 4. Adsorption isotherm determination

The application of the techniques summarized in Section 3.2 to the experimental results reported in Section 3.1 requires knowledge of the adsorption isotherms characterizing the system under consideration. Therefore, the objective here is to describe the adsorption equilibria using one of the adsorption

isotherms referred to above, on the base of a few measurements made using the racemate and not the pure components, which were still unavailable at this stage. This is a rather typical situation when dealing with the separation of high value pharmaceutical products. In this case a three step procedure has been adopted: first the Henry constants have been determined; secondly one of the adsorption isotherm has been selected and its parameters have been estimated; finally these have been fine tuned using the results of a few experiments on the SMB unit itself.

##### 4.1. Henry constant determination

Henry constants,  $H_i$ ,  $i = A, B$ , can be determined by measuring the retention time of a pulse of the relevant species under linear conditions, i.e., at infinite dilution. Under such conditions competition is absent and chromatograms using the racemate provide the same information as those using the pure enantiomers.

The following parameters have been defined:

- Observed retention time,  $t_{R,i}$ , which is a function of the Henry constant of the  $i$ -th component through the following relationship:

$$t_{R,i} = t_D + (t_0 - t_D) \left( 1 + \frac{1 - \varepsilon}{\varepsilon} H_i \right). \quad (2)$$

- Residence time,  $t_0$  (this corresponds to the observed retention time of a non-retained species and allows the calculation of the bed void fraction):

$$t_0 = t_D + \frac{\varepsilon V}{Q}. \quad (3)$$

- Extra-column dead time,  $t_D$  ( $V_D$  is the extra-column dead volume):

$$t_D = \frac{V_D}{Q}. \quad (4)$$

The following values have been measured on the analytical column:  $t_D=0.56$  min;  $t_0=3.72$  min, hence  $\varepsilon=0.704$ ;  $t_{R,A}=8.35$  min and  $t_{R,B}=5.60$  min. The more retained enantiomer labelled A corresponds to (*S*)-(+)-guaifenesin, whereas the less retained enantiomer, B, is (*R*)-(-)-guaifenesin. From these values the following Henry constants of the

two enantiomers have been calculated:  $H_A = 3.49$  and  $H_B = 1.41$ . It is worth noting that the Henry constants are scalable quantities, which can be used to predict the chromatographic behavior of the two enantiomers in a different column packed with the same stationary phase and operated with the same mobile phase at the same temperature; in particular this applies to the columns of the SMB unit. From Eq. (2) dimensionless values of the Henry constants are obtained. Since in the SMB unit the same stationary phase and packing procedure have been adopted, it is assumed that the void fraction of the SMB columns is the same as that of the analytical column.

A final remark concerns the fact that the value of the Henry constants is a function of the extra column dead volume, which must be carefully measured. On the contrary the selectivity, i.e., the ratio of the values of the two Henry constants, is independent of this value.

#### 4.2. Estimation of Langmuir equilibrium constants

A limited number of pulse chromatograms with different injected amounts (see Fig. 3) were available for the determination of the nonlinear multicomponent isotherm. The shape and elution time of the pulses are influenced by the competitive adsorption isotherms and by the mass transfer and axial disper-

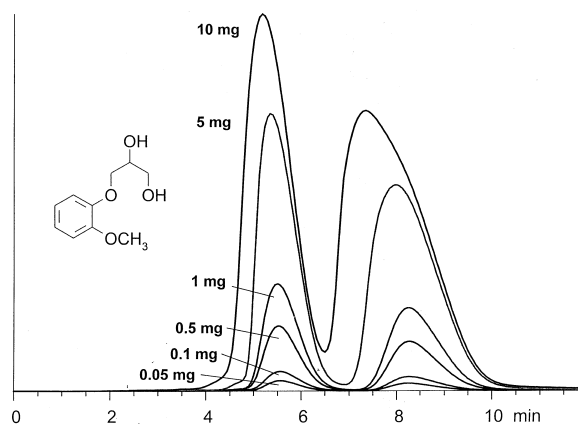


Fig. 3. Pulse chromatograms of the enantiomers of guaifenesin at increasing loaded amount. Column geometry and operating conditions as in Section 2.1; the amount indicated in the plot refers to the racemate.

sion phenomena in the column. In principle, a detailed model of the chromatographic column could be used to simulate these chromatograms and determine through a fitting procedure the isotherm parameters. However, this approach requires more information to be really effective. Note in particular that the chromatograms corresponding to 0.05 to 1 mg of injected racemate exhibit a quasi-linear behavior and cannot be used for the nonlinear parameter estimation.

Therefore, a simplified approach was adopted based again on the equilibrium theory model and assuming that the multicomponent Langmuir isotherm could be used to describe the system. If the three isotherms mentioned above (Langmuir, modified Langmuir and bi-Langmuir) are regarded simply as empirical relationships, the Langmuir isotherm is the one with the least number of parameters and is the recommended choice when scarce equilibrium information are available. In this case, since the Henry constants of the enantiomers were measured precisely, only two parameters—one for each enantiomer—are still to be estimated.

This was done on the basis of the two chromatograms at 5 and 10 mg loading, following the procedure described by Guiochon et al. [15]. Each chromatogram yields a pair of values of the Langmuir equilibrium constants (one prime and two primes correspond to the 5 mg and the 10 mg chromatogram, respectively):  $K'_B = 0.0125$  1/g;  $K''_B = 0.0145$  1/g;  $K'_A = 0.014$  1/g;  $K''_A = 0.028$  1/g. The values referring to the weak component are satisfactorily consistent whereas those of the strong enantiomer indicate a rather poor fitting. If these values are averaged the following competitive Langmuir isotherms are obtained:

$$q_A = \frac{3.5c_A}{1 + 0.021c_A + 0.0135c_B}$$

$$q_B = \frac{1.4c_B}{1 + 0.021c_A + 0.0135c_B} \quad (5)$$

The fluid and adsorbed phase concentrations have units of g/l; the reference volume is the fluid phase volume for the former and the solid-phase volume (true solid volume excluding pores inside the particle) for the latter.

#### 4.3. Tuning of adsorption isotherm parameters

The isotherms (Eq. (5)) clearly provide only a rough description of the true competitive behavior of the two enantiomers. In order to improve the accuracy of the thermodynamic model more experiments and a more detailed fitting procedure would be needed. Alternatively, it is possible to tune the equilibrium isotherm parameters on the basis of a small set of SMB experiments. This is consistent with the ultimate reason of looking for an adsorption equilibrium model, i.e., the objective of explaining and predicting the behavior of the laboratory SMB unit used to perform the experiments reported in Section 3.1.

To this aim runs F1 to F7 have been considered (see Table 1). First, the complete separation region corresponding to the Langmuir isotherm (Eq. (5)) has been drawn in Fig. 4 (dashed boundaries), together with the operating points corresponding to the experimental runs. These share the same value of  $m_2$ , whereas they have increasing values of  $m_3$  for increasing values of the feed flow-rate (see Table 1). Therefore they are located on a vertical straight line in the  $(m_2, m_3)$  plane, and lie within the complete

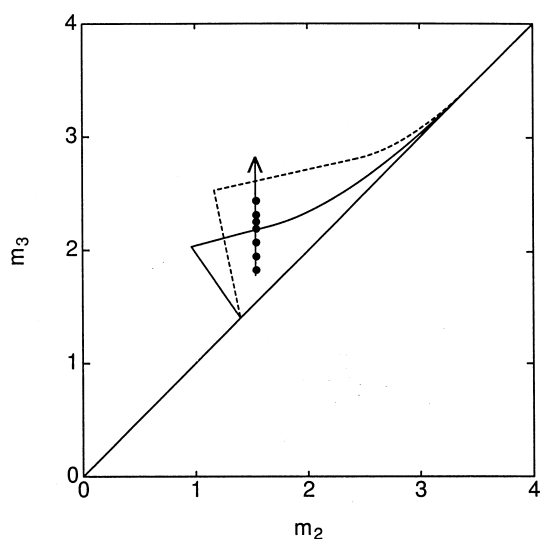


Fig. 4. Separation of guaifenesin enantiomers in the pilot SMB unit. Region of complete separation: (---) isotherms given by Eq. (5); (—) isotherms given by Eq. (6). (●): Operating points corresponding to runs F1 to F7 in Table 1 (F1 and F7 are the lowest and the highest point, respectively).

separation region. This is clearly inconsistent with the experimental purity values which indicate that the operating points of runs F5 to F7 should lie within the pure extract region. It is worth noting that this conclusion is correct since in all the experimental runs reported in Table 1 the flow-rate ratio in section 1,  $m_1$  is larger than its critical value, which corresponds to  $H_A$ , i.e., in all cases  $m_1 > 3.5$ .

The tuning of the adsorption isotherm parameters is performed so as to make the complete separation region consistent with the position of the operating points and the corresponding experimental performances. This can be achieved by letting the parameter  $K_B$  constant and equal to 0.0135, while changing  $K_A$ , whose estimation in the previous section was rather uncertain. The newly obtained value is  $K_A = 0.055$ , thus yielding the following isotherms:

$$q_A = \frac{3.5c_A}{1 + 0.0550c_A + 0.0135c_B}$$

$$q_B = \frac{1.4c_B}{1 + 0.0550c_A + 0.0135c_B} \quad (6)$$

The corresponding complete separation region is also drawn in Fig. 4 (solid boundaries) and now the agreement between theory and experiments is evident. It is worth noting that this figure provides a clear understanding of the reason why changing the feed flow-rate has a detrimental effect only on the raffinate purity, while on the other hand the extract purity remains very close to 100%. For the adopted values of all the other parameters, the change of the feed flow-rate can only make the operating point of the SMB unit switch between the complete separation region and the pure extract region along the same vertical line in the  $(m_2, m_3)$  plane without spoiling the extract purity.

The overall picture of all the four regions of separation for the adopted isotherms is illustrated in Fig. 2.

#### 5. Analysis of experimental results

The approach applied so far, involving the determination of the adsorption isotherms (Eq. (6)) through fitting of some SMB experiments, can prove

its value and usefulness by comparison with all the other available SMB experimental results.

### 5.1. Effect of extract flow-rate

With reference to runs E1 to E7 in Table 1 it can be noted that the increase of the extract flow-rate yields a decrease of both  $m_2$  and  $m_3$ . As illustrated in Fig. 5 the corresponding operating points lie on a straight line of unitary slope which crosses the complete separation region. In full agreement with the experimental purity values the points E1 and E2 lie in the pure extract region whereas points E6 and E7 lie in the pure raffinate region. Finally points E3 to E5 are within the complete separation region.

### 5.2. Experiments G1 to G5

Despite the changes in all four operating parameters, i.e.,  $t^*$ ,  $Q_1$ ,  $Q_E$  and  $Q_F$ , experiments G1 to G5 have very similar values of the flow-rate ratios  $m_2$  and  $m_3$ , which are very close to those of runs F4 and E3 too. The operating points of all these runs coincide and fall within the complete separation

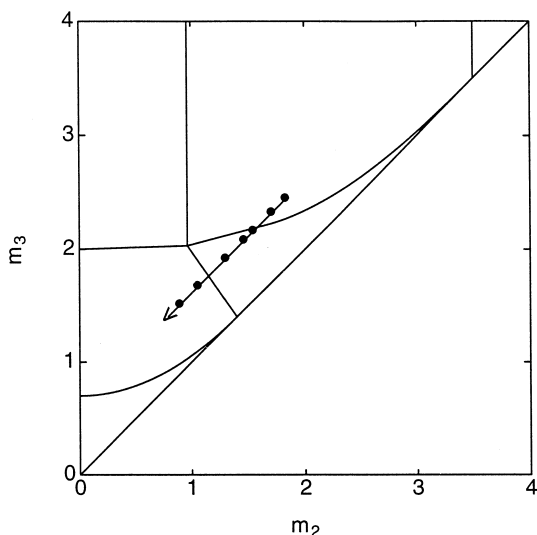


Fig. 5. Separation of guaifenesin enantiomers in the pilot SMB unit: effect of changing the extract flow-rate. (—) Region of complete separation. (●): Operating points corresponding to runs E1 to E7 in Table 1 (E1 and E7 are the rightmost and the leftmost point, respectively).

region. Accordingly, as reported in Table 1, the corresponding experimental purity values are very close to each other.

It is worth mentioning a minor effect which is exhibited by this set of experiments. It can be noticed that the flow-rate ratio in section 1 decreases in going from run G1 to run G5. Even though in all cases it is larger than the critical value, i.e., 3.5, when this parameter gets closer and closer to its lower bound the band broadening effect of axial dispersion and mass transfer resistances becomes more and more important. This can make the regeneration of the stationary phase performed in section 1 less and less effective, thus hindering raffinate purity. This effect is evident if one looks at runs G1 to G5, where  $P_R$  decreases steadily from 99.7% when  $m_1 = 4.32$  to 99.2% when  $m_1 = 3.92$ . However, it is even more impressive if one considers also run F4, which achieves 99.7% raffinate purity with  $m_1$  as large as 4.58, and run E3, where  $P_R$  is only 99.1% and  $m_1 = 3.76$ , which is the smallest value among those considered here.

### 5.3. Effect of feed flow-rate and optimization

Let us refer again to Fig. 4. If feed flow-rates were increased further beyond the maximum experimental value of 0.70 ml/min (run F7), extract purity would not be hindered. If the more retained enantiomer were the only one of interest and raffinate purity were not one of the objectives of the separation, we could wonder whether productivity could be improved with no limits by choosing operating points further and further along the vertical straight line to which operating points F1 to F7 belong. To verify this, a proper performance parameter representing the productivity of the more retained component should be defined:

$$PR_A = \frac{c_A^E Q_E}{N_c V \rho_s (1 - \varepsilon)} \quad (7)$$

The extract concentration  $c_A^E$  was not available after these experiments, and therefore it was not possible to calculate the experimental values of  $PR_A$ . However, some simulations have been made using a model of the SMB unit based on equilibrium theory. The results are reported in Fig. 6 in terms of purities



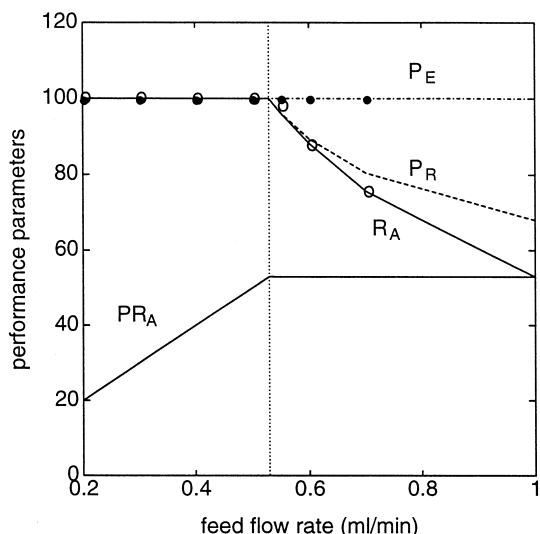


Fig. 6. Separation of guaifenesin enantiomers in the pilot SMB unit: effect of changing the feed flow-rate. (— · —) Extract purity; (— · —) raffinate purity; (—) recovery of A in the extract; (—) normalized value of the productivity of A, defined by Eq. (7); (· · ·) critical value of the feed flow-rate indicating the boundary between the complete separation and the pure extract region. Experimental runs F1 to F7 in Table 1: (●) extract purity; (○) raffinate purity.

of the outlet streams, recovery (percentage of A recovered in the extract with respect to the amount fed to the SMB unit) and productivity of the more retained enantiomer,  $PR_A$ , as a function of the feed flow-rate (keeping all the other parameters constant). It can readily be observed that the agreement between measured values (referring to runs F1 to F7) and calculated ones of the outlet purities is qualitatively good and quantitatively satisfactory. The decrease of the calculated value of the recovery parameter outside the complete separation region (its boundary is indicated by the dotted vertical line in the figure) is a consequence of the loss of raffinate purity. The behavior of the parameter  $PR_A$ , which is maximum on the boundary of the complete separation region and remains constant beyond it, is remarkable and indicates that no further improvement can be achieved outside the complete separation region in terms of productivity of the desired enantiomer. Within the complete separation region increasing the feed flow-rate yields an improvement

of the productivity of both enantiomers, since the operating conditions allow separation of the two components. On the contrary, outside the complete separation region any further amount of A fed to the unit is collected in the wrong outlet stream, thus hindering raffinate purity and yielding no effect on the productivity of A.

It can be concluded that optimizing the operating conditions of a SMB unit implies remaining within the complete separation region even when the recovery of only one of the products to be separated is the aim. In the frame of equilibrium theory also in this case optimal operating conditions correspond to the vertex of the triangle shaped complete separation region in Fig. 2. It can be easily demonstrated that this result bears general validity.

## 6. Notation

$c$	fluid phase concentration
$H$	Henry constant
$K$	Langmuir adsorption equilibrium constant
$m_j$	flow-rate ratio in section $j$ , defined by Eq. (1)
$N_c$	number of columns in the SMB unit
$P$	desorbent free purity
$q$	adsorbed phase concentration
$Q$	volumetric flow-rate
$PR$	productivity, defined by Eq. (7)
$t_D$	extra-column dead time, defined by Eq. (4)
$t_R$	observed retention time, defined by Eq. (2)
$t_0$	residence time, defined by Eq. (3)
$t^*$	switch time in a SMB unit
$V$	volume of the column
$V_D$	extra-column dead volume

### Greek letters

$\varepsilon$	overall void fraction of the bed
$\rho_s$	bulk stationary phase mass density

### Subscripts and superscripts

A	more retained enantiomer
B	less retained enantiomer
E	extract
F	Feed
$i$	component index
$j$	section index
R	raffinate

## References

- [1] D.M. Ruthven, C.B. Ching, *Chem. Eng. Sci.* 44 (1989) 1011.
- [2] J.N. Kinkel, M. Schulte, R.M. Nicoud, F. Charton, in: *Proceedings of the Chiral Europe '95 Symposium*, Spring Innovations Limited, Stockport, UK, 1995, p. 121.
- [3] M.J. Gattuso, B. McCulloch, J.W. Priegnitz, *Chem. Tech. Europe* 3(3) (1996) 27.
- [4] M. Negawa, F. Shoji, *J. Chromatogr.* 590 (1992) 113.
- [5] C.B. Ching, B.G. Lim, E.J.D. Lee, S.C. Ng, *J. Chromatogr.* 634 (1993) 215.
- [6] R.-M. Nicoud, G. Fuchs, P. Adam, M. Bailly, E. Küsters, F.D. Antia, R. Reuille, E. Schmid, *Chirality* 5 (1993) 267.
- [7] E. Küsters, G. Gerber, F.D. Antia, *Chromatographia* 40 (1995) 387.
- [8] F. Charton, R.-M. Nicoud, *J. Chromatogr. A* 702 (1995) 97.
- [9] S. Nagamatsu, K. Murazumi, H. Matsumoto, S. Makino, in: *Proceedings of the Chiral Europe '96 Symposium*, Spring Innovations Limited, Stockport, UK, 1996, p. 97.
- [10] L.S. Pais, J.M. Loureiro, A.E. Rodrigues, *Chem. Eng. Sci.* 52 (1997) 245.
- [11] D.W. Guest, *J. Chromatogr. A* 760 (1997) 159.
- [12] E. Francotte, P. Richert, *J. Chromatogr. A* 769 (1997) 101.
- [13] M. Mazzotti, M.P. Pedferri, M. Morbidelli, Design of optimal and robust operating conditions for chiral separations using simulated moving beds, in: *Proceedings of the Chiral Europe '96 Symposium*, Spring Innovations Limited, Stockport, UK, 1996, p. 103.
- [14] M. Mazzotti, G. Storti, M. Morbidelli, *J. Chromatogr. A* 769 (1997) 3.
- [15] G. Guiochon, S. Golshan-Shirazi, A.M. Katti, *Fundamentals of Preparative and Nonlinear Chromatography*, Academic Press, Boston, 1994.
- [16] J.W. Priegnitz, Small scale simulated moving bed separation apparatus and process, U.S. Patent 5 470 464, November 28, 1995.
- [17] A. Gentilini, C. Migliorini, M. Mazzotti, M. Morbidelli, *J. Chromatogr. A*, submitted.